Magnetic properties of Fe nanoclusters: *ab initio* calculations of Fe_N, N = 9, 15, 27, 51, and 59

G. López Laurrabaquio and M. Pérez Alvarez
Instituto Nacional de Investigaciones Nucleares,
Km 36.5, Carretera México-Toluca, Ocoyoacac, Estado de México 52045, México,
e-mail: gll@nuclear.inin.mx

J.M. Montejano-Carrizales
Instituto de Física, Universidad Autónoma de San Luis Potosí,
76240, San Luis Potosí, México,
e-mail: jmmc@ifisica.uaslp.mx

F. Aguilera-Granja*
Departamento de Física Teórica, Atómica, y Óptica, Universidad de Valladolid,
E-47011, Valladolid, Spain.

J.L. Morán-López
Instituto Potosino de Investigación Científica y Tecnológica,
78216, San Luis Potosí, México,
e-mail: moran-lopez@ipicyt.edu.mx

Recibido el 9 de febrero de 2006; aceptado el 19 de junio de 2006

The magnetic properties of iron clusters (Fe_N, $N = 9$, 15, 27, 51, and 59 atoms) at $T = 0$ K with bcc-like structure and bulk parameters are studied using *ab initio* methods. In these studies we consider the spin-orbit coupling and applied external magnetic fields. The basis set includes wave functions of the *s*, *p*, *d*, and *f* valence electrons. An analysis of the spin and orbital magnetic moments for every shell of the different cluster sizes is performed. The results obtained in the present work agree with other results reported in the literature and call for additional experiments.

Keywords: Magnetic nanostructures; magnetic properties; *ab initio* calculations.

Se estudian las propiedades magnéticas de cúmulos de hierro (Fe_N, $N = 9$, 15, 27, 51, y 59 átomos) a $T = 0$ K y con estructura bcc, parámetros de bulk y usando métodos *ab initio*. En este estudio se considera el acoplamiento espín-orbita y se aplica un campo magnético externo. La base incluye funciones de onda de los electrones de valencia *s, p, d,* y *f*. Se lleva a cabo un análisis de los momentos magnéticos de espín y orbital para cada capa de los diferentes cúmulos considerados. Los resultados obtenidos aquí están están en acuerdo con otros resultados reportados en la literatura y provoca la realización de experimentos adicionales.

Descriptores: Nanoestructuras magnéticas; propiedades magnéticas; cálculos *ab initio*.

PACS: 75.50.-y; 75.50.Bb; 36.40.Cg

1. Introduction

It has long been observed that the effective magnetic moment per atom in very small clusters is greater than the bulk value and that they behave as superparamagnetic clusters at thermal equilibrium conditions [1]. The magnetic moment of free $3d$-transition-metal clusters has been measured by de Heer *et al.* [2–4] and by Bloomfeld *et al.* [5–7] by means of Stern-Gerlach experiments. They have observed that the magnitude of the average magnetic moment per atom in small clusters is close in magnitude to that of the isolated atom. As the cluster size increases, the average magnetic moment decreases and oscillates. Finally, the bulk value is achieved for clusters with sizes of the order of 700 atoms. They have also shown that the magnetic field- and the temperature-dependence of the average magnetic moment are expressed by the Langevin type function for non-interacting atoms.

In addition to the global features mentioned above, there are other interesting features in the magnetism of clusters. Billas *et al.* [3] suggested the existence of a geometrical magnetic shell, in which the local magnetic moment changes shell, by shell from the surface to the inner region of the clusters.

There have been various theoretical reports trying to explain the experimentally observed features. The problem is complicated since there is no experimental information on the geometrical characteristics of the small clusters. There is also no information about the geometrical characteristics as a function of the size. In view of this lack of information, one generally assumes that the geometry adopted by the clusters is the same as the bulk crystalline lattice. Thus, in the case of Fe, one assumes that the clusters grow as small chunks of a bcc lattice and that Ni clusters follow the fcc structure. Given these assumptions, one must choose the theoretical model

and approximations needed to calculate the electronic and magnetic structure. The results obtained through this line of reasoning are already a good starting point for learning about the physicochemical properties of clusters as a function of size.

However, the geometrical structure of free standing clusters must be determined by the minimization of the total energy ruled by the electronic structure. To carry out this procedure, one must perform *ab initio* all electron calculations and minimize the energy as a function of the geometrical arrangement and interatomic distances. There have been some reports on first principle studies for relaxed clusters [8–12]. For small clusters Fe_N, $N \leq 7$, it has been found by means of a density functional theory calculation that Jahn-Teller distortions stabilize open structures that differ from the bcc structure. The comparison of these results with photoelectron spectroscopy studies [13] seems to validate these geometrical arrangements.

For larger clusters, it has been reported that Fe_{13} could take on the geometry of a distorted iscosahedron. One can also obtain different magnetic orderings, *i.e.* ferromagnetic or antiferromagnetic. This is understandable since, as the cluster size grows, one must sample a manifold energy surface where the minima are very shallow. That is why with, the actual computational facilities and codes, the clusters that can be calculated consist of a small number of atoms.

From bulk and surface studies one knows that the electronic and therefore the magnetic properties of transition metal atoms depend strongly on the environment; *i.e.* the local magnetic moment of a particular atom depends strongly on its coordination number and on what kind of neighbours it has. In CuNi alloys for example, the existence of magnetic moments in the Ni atoms depends on the number of nearest Ni neighbours, which in turn depends on nominal alloy concentration [14].

In the same way, one expects that the magnetic properties of transition metal clusters will depend strongly on the geometrical structure and that each one of the atoms composing the cluster will possess magnetic moments that depend on the local environment. For example, in a cluster of 9 Fe atoms in a bcc geometry, the central atom, which has its nearest neighbour a complete shell (8 atoms), will possess a magnetic moment that is different from the other 8 which are single-coordinated to the central atom. To build the next shell, one needs 6 atoms. In this new cluster, the first shell atoms now get three neighbours in the second shell and are now 4-coordinated. The six atoms of the second shell also have 4 nearest neighbours.

In view of these special cluster characteristics, several authors have explained the oscillatory behaviour in the average magnetic moment as a function of size by means of shell models [4, 15–17]. These models give an oscillatory behaviour in the average magnetic moment but differ from the experimentally observed behaviour. More recently, an *ab initio* calculation of the magnetic structure of small iron clusters has been reported [18]. They calculate the local spin and orbital magnetic moments and find a linear dependence on the effective coordination number.

In the present work, taking into account the complexity of the problem and being interested in the main trends of the orbital magnetic moment and the effect of applied magnetic fields, we calculate at 0K the magnetic properties of iron atom clusters made of 9, 15, 27, 51, and 59 atoms with a bcc structure. The lattice parameters are set equal to the bulk values. We are aware that this assumption for the clusters with 9 and 15 atoms may not be the correct one, but we do it in order to get the complete sequence of bcc clusters. There are indications that clusters with $N > 25$ adopt the bcc structure [19].

The electronic calculations are done using the Cerius [20] code, which is an *ab initio* method; within this method we calculate the spin and orbital magnetic moments. In addition, the 59-atom cluster is immersed in a magnetic field, and the induced magnetic moments are calculated.

In these calculations, we include the spin-orbital interaction and analyze the spin and orbital magnetic moments for every shell of the clusters. We also study the orbital angular momentum projection of the electronic charge distribution in each atom in different shells, particularly in the surface shell and in the central atom. We calculated the total charge at each site, *i.e.* the sum of spin-up and spin-down valence electrons. Thus, we analyze the cooperative phenomenon and local atomic structure.

This work is organized as follows: in Sec. 2, a brief description of the calculation is given. In Sec. 3, we present the results and the discussion of the calculations of the orbital and spin magnetic moments for the different shells and clusters sizes. Later, we study the effect of applied fields on the orbital and spin magnetic moments for the 59-atom cluster. Finally, the conclusions are presented in Sec. 4.

2. Model and calculation

2.1. Geometrical Characteristics

As mentioned above, one key factor determining the physicochemical properties of nanoclusters is their geometric arrangement. In particular, the geometrical structure is of major importance in determining the magnetic properties. Therefore, we first describe the geometrical characteristics of the clusters studied here. In Fig. 1a we show the 27-atom cluster with bcc structure. The hatched circle is the central atom, and is denoted as the zero site. Shell one consists of the first eight neighbors beside the central atom and these are shown as black circles. Shell two contains the next six neighbors, shown as gray circles, which are four-fold coordinated with the first shell atoms. Finally the outermost external shell, the third one, consists of 12 atoms (in white), two-fold coordinated with the second shell atoms.

Figure 1b shows the 59-atom cluster. The hatched circles correspond to the 27 cluster, discussed above. The 24 atoms

in the fourth shell are shown as gray circles, and the outermost shell, the fifth, which contains 8 atoms, is shown by open circles. The full information on the geometrical characteristics is contained in Table I, where the first column shows the number of atoms in the various shells. The second column shows the shell number, and the matrix elements a_{ij} are the coordination numbers of an atom in shell i to atoms located in shell j. This information is vital to understanding the magnetic structure of clusters.

TABLE I. Geometrical structure of bcc clusters. The first column is the total number of atoms in the various shells denoted in column 2. The matrix elements a_{ij} are the coordination numbers of an atom in shell i to atoms located in shell j.

	$i\backslash j$	0	1	2	3	4	5
1	0	0	8	0	0	0	0
8	1	1	0	3	3	0	1
6	2	0	4	0	0	4	0
12	3	0	2	0	0	4	0
24	4	0	0	1	2	0	1
8	5	0	1	0	0	3	0

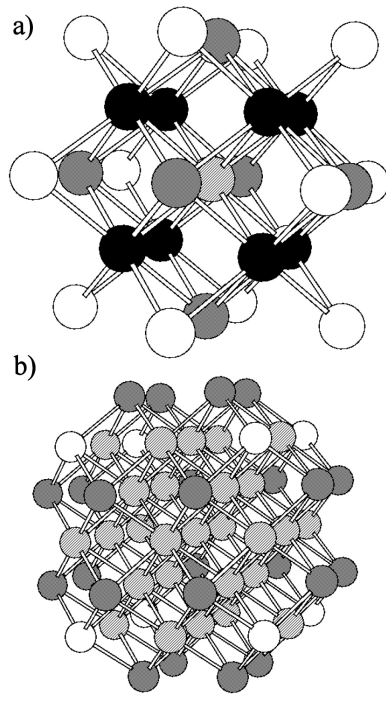

FIGURE 1. a) The 27 atom cluster with bcc structure. The hatched circle is the central atom. Shell one consists of the first eight neighbors beside the central atom and these are shown as black circles. Shell two contains the next six neighbors, shown as gray circles. The outermost shell consists of 12 atoms (in white). b) The 59-atom cluster with bcc structure. The hatched circles correspond to the 27 cluster. The 24 atoms in the fourth shell are shown as gray circles, and the outermost shell, the fifth, that contains of 8 atoms is shown by open circles.

2.2. Computational Procedure

The Cerius [20] code used in the present calculation consists of several modules. The one implemented in this work was the ESOCS [21–23] (Electronic Structure of Close-packed Solids). It is a code that is based on first quantum mechanical principles and has been used to calculate the electronic structure of the surfaces and bulk of a wide range of solid-state systems, including metals and semiconductors. It is important to mention that this code includes the spin-orbital coupling.

This code was developed to study systems with periodic boundary conditions. Thus, one can study an infinite piece of matter, at a calculation cost that is determined by the number of atoms in the unit cell. Defect structures, surfaces, clusters, and even molecules can be studied by imposing periodic boundary conditions, by generating supercells that contain the object of interest. ESOCS transforms the conventional cell to the primitive calculation cell. The calculation time per k-point in an ESOCS run ranges scales between the square and the cube of the number of the atoms in the cell.

ESOCS is based on the spin functional density and the atomic sphere approximation, ASA. The main characteristic of this code is an expansion in spherical waves of the wave functions, which are centered in each atomic site. Due to this construction, the projection of the quantities such as electronic densities of states, charge, spin and orbital magnetic moment onto atomic sites is easily calculated.

The basis wave-function set used by ESOCS is the solution of the Schrödinger equations for energies in the valence region, which are automatically orthogonal to all the on-site core orbitals. Thus, every basis wave-function is orthogonal to all core orbitals of the system [23]. The Bloch functions of the system are then expanded in this basis set. One vital feature that greatly improves the calculation efficiency is that each basis function, regardless of which atom it is centered on, is orthogonal to all core levels of the entire crystal.

A second approximation that is imposed by ESOCS is the use of a single basis function per atom per partial wave. In this code, it is assumed that the crystal is a close-packed metal, and under this assumption, it takes the next upper orbital from the valence states and it is added to the basis wave-function set.

By taking into account these two approximations, for the case of the Fe, Cerius uses the basis set $4s4p3d$. The $4s3d$ states result from the first approximation and the wave-function corresponding to $4p$ results from the second one. This is named the polarization function. The principal quantum number for this basis set is $n = 4$. Furthermore, the polarization function has an orbital angular moment higher than the one for the atomic functions associated with the occupied levels in the atom. Then the values $L = 0$, 1, 2, and 3 are the values of the projection of the orbital angular moment.

To implement the ESOCS code for the study of the magnetic properties of the Fe aggregates, the cluster is located inside a "primitive cell", taking into account the initial conditions previously indicated; *i.e.* the size the primitive cell

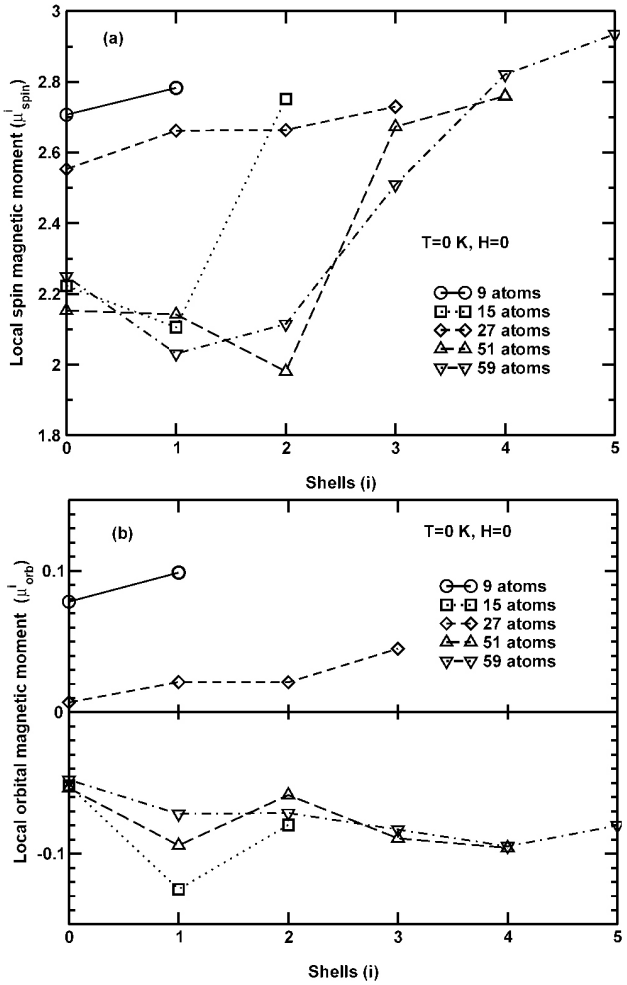

FIGURE 2. The spin (a) and the orbital (b) magnetic moment for atoms located at the various neighbor shells and for different cluster sizes. Site zero is the central atom. In this calculation, $H = 0$ and $T = 0$.

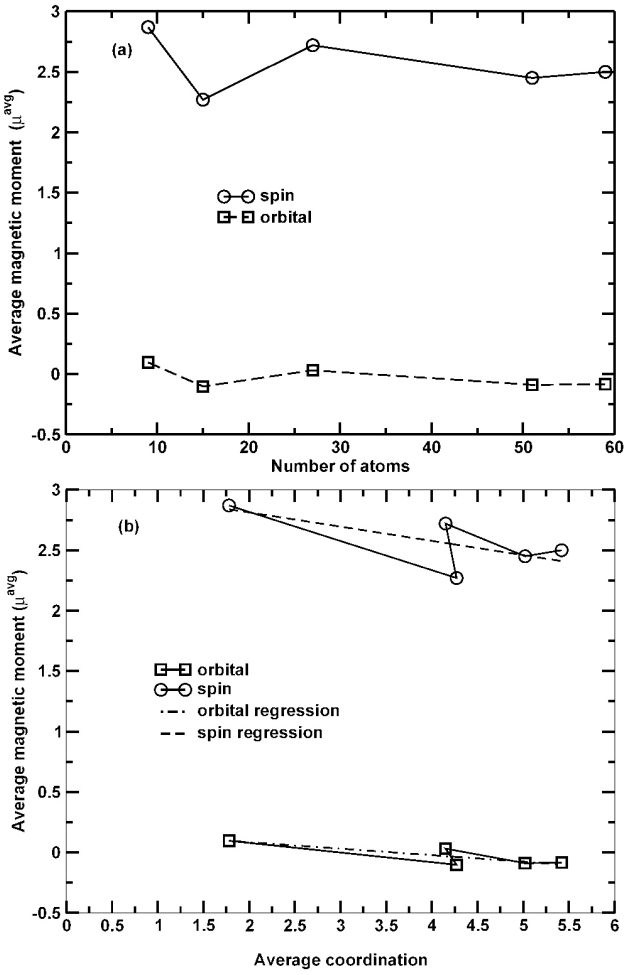

FIGURE 3. The average spin and orbital magnetic moments as: a) a function of the number of the atoms in the cluster and b) a function of the average coordination number in the cluster.

will be determined under the following criteria: a) the total energy has a minimum, b) the values of the spin and orbital magnetic moments at the center of the cluster approach bulk values and those on the cluster surface, values of a thin film, and c) the primitive cell size is such that, when applying the atomic sphere approximation, ASA, the overlap is minimum.

3. Results and discussion

The results obtained for the spin and orbital magnetic moment for atoms located in the various shells and for different cluster sizes, $H = 0$ and $T = 0$ K, are shown in Figs. 2a and 2b. As mentioned above, the numeration of the shells is in increasing order with respect to the distance from the center of the cluster.

The largest value for the average of the spin magnetic moment per atom is obtained for the smallest cluster, in which the central atoms possess a $\mu_S = 2.73$ Bohr magnetons and the surface atoms $\mu_S = 2.78$. In this cluster, the central atom has eight neighbors and the surface atoms are only single bonded to the central one. In the next cluster size, obtained by adding 6 atoms, the number of bonds increases substantially, since the central atoms has its 8 neighbors, the atoms in the first shell are now four-fold coordinated (instead of monocoordinated) and the outermost atoms are also four-coordinated. This effect means that the central atom attains a spin magnetic moment value very close to the bulk one, the first shell atoms show a magnetic moment smaller that the central atom, and the outermost atoms have a large spin magnetic moment, similar to the surface atoms of the 9-atom cluster. It is important to note that this kind of oscillation is typically due to the charge oscillations near a surface. These results make evident how sensitive the electronic structure is on the geometrical structure.

The cluster with 27 atoms, whose geometrical structure was discussed above, has a more open geometrical structure in which 12 of the 27 atoms are only two-fold coordinated. With slight oscillations, the spin magnetic moment shows values similar to the 9-atom cluster. Adding 24 and 32 atoms, the magnetic moment structure resembles more a core similar to bulk iron and an enhanced magnetic moment at the surface atoms.

The results for the orbital magnetic moment are shown in Fig. 2b. The trends are similar to the spin magnetic moments with the observation that we obtain negative values for the cases of the clusters with 15, 51 and 59 atoms. As expected, the absolute values are very small compared to the spin magnetic moments.

As far as the calculations of magnetic moments is concerned, an interesting and important aspect is the almost alternation of the signs of the orbital magnetic moments as the cluster size grows. This is due to the fact that spin and orbital magnetic moments are combined to achieve the most stable configuration of the cluster.

Table II shows the values of the contributions resulting from the various electron orbital angular moments (s, p, d and f), to the total value of the spin moment, defined as the difference between the spin-up and spin-down valence electrons. This information is given for the central and outermost atoms. The table also contains the values of the contributions to the total electronic charge, which is the sum of the spin-up and spin-down valence electrons. Table II also shows the total charge difference between the surface shell and the central atom, ΔQ.

As expected, from the numerical results, it can be seen that the most important contribution to the spin magnetic moment arises from the projection of the orbital angular moment with $L = 2$. The second important contribution comes from p, and the smallest contribution is due to the s electrons. The $3d$- and $4s$ valence electrons in atomic Fe redistribute themselves and partially occupy the p and f levels.

TABLE II. Contributions to the local spin magnetic moment and the local charge of atoms at the center and the surface, arising from different orbitals (s, p, d, and f), for the various cluster sizes. The last column gives the charge difference between the central and surface atoms.

Cluster	Electronic charge projection	Local spin magnetic moment		Charge		ΔQ
		Center	Surface	Center	Surface	
	d	2.59106	2.71676	6.52362	6.52132	
Fe_9	s	-0.02214	-0.00145	0.81156	0.74001	
	p	0.07830	0.03275	0.71470	0.63969	
	f	0.05995	0.03456	0.10954	0.07906	
	total	2.70717	2.78262	8.15942	7.98008	0.17934
	d	1.59370	2.07813	5.52913	4.41826	
Fe_{15}	s	0.02072	0.09940	0.98742	0.90959	
	p	0.30686	0.30432	2.15246	1.44678	
	f	0.30155	0.26989	2.52207	2.37377	
	total	2.22283	2.75174	11.19108	9.14840	2.04268
	d	2.47841	2.53695	5.78612	6.21471	
Fe_{27}	s	-0.02143	0.42145	0.71915	0.81029	
	p	0.02000	0.09741	0.88094	0.90363	
	f	0.07565	0.06338	0.32549	0.77069	
	total	2.55263	2.73035	7.71170	8.69932	-0.98762
	d	1.76812	2.43788	5.42262	4.34758	
Fe_{51}	s	-0.01660	0.03112	0.98421	0.74778	
	p	0.25618	0.16795	1.77086	0.94333	
	f	0.14538	0.12323	1.51722	1.51459	
	total	2.15308	2.76018	9.69491	7.55328	2.14163
	d	1.93176	2.66666	5.35918	4.58928	
Fe_{59}	s	-0.02673	0.01954	1.00515	0.73410	
	p	0.22200	0.12518	1.69356	0.83802	
	f	0.12350	0.12389	1.81756	1.34343	
	total	2.25053	2.93527	9.87545	7.50483	2.37062

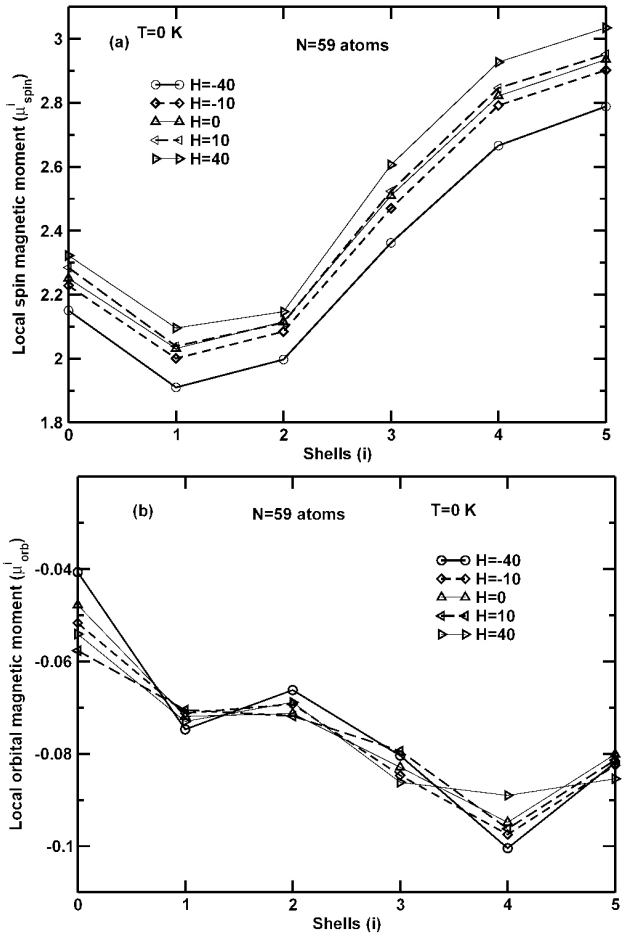

FIGURE 4. The local spin (a) and orbital (b) magnetic moments for atoms at the various shells, for the 59-atom cluster, for several values of the applied magnetic field H.

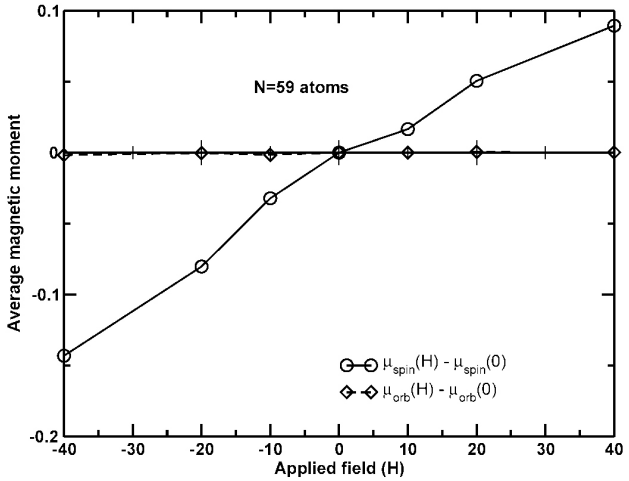

FIGURE 5. The average spin and orbital magnetic moments of the 59-atom cluster as a function of the applied magnetic field, referred to the values for $H = 0$.

The average spin and orbital magnetic moments as a function of the number of atoms in the cluster is shown in Fig. 3a. Similar behavior was obtained by Franco [15] and Guevara [24] using tight binding models. The trends are similar to those observed experimentally [2–4], but it is difficult to compare them with our results since the magnetic moment reported from experiments are for larger clusters and there are large error bars for the clusters 10 atoms. Furthermore, the estimated temperature at which the clusters were measured is 120 K.

In Fig. 3b, the average spin and orbital magnetic moment as are shown a function of the average coordination number in the various clusters. To explain the decrease in the spin magnetic moment as a function of the average coordination number, several geometrical shell models have been proposed [3, 16, 17], where the magnetic moments of a particular atom are determined by its coordination number.

We compared the electronic local density of states measured by photoelectron spectroscopy studies [13] with our results for the clusters with 9, 15 and 27 atoms. Athough a direct comparison cannot be made, since the experimental results are obtained for charged particles, the main features for the 9-and 27-atom clusters are reproduced. This means that the geometrical structure is not too different from the bcc structure that was assumed in the calculation. That is not the case for the 15-atom clusters where there are substancial differences. A more detailed analysis on this issue will be published elsewhere.

Finally, the 59-atom cluster is embedded in an external magnetic field in the range between -40kG and $+40$kG at temperature T=0 K. Fig. 4 shows some results of the spin and orbital magnetic moments for several values of the applied magnetic field. The behavior of the spin magnetic moment, when applying the magnetic field in the positive direction of z, shows an increment in each shell and the opposite occurs when it is applied in the negative direction, as was to be expected. The lines drawn through the various shells are not parallel and show an effect that is produced by the interplay of all the electrons. This effect is known as the Pauli paramagnetism and the increase (or decrease for negative fields) is proportional to the difference in population of electrons with opposite spins.

The orbital magnetic moment has a peculiar behavior. This is due to the fact that the orbital momentum reacts to the application of an external field producing a diamagnetic effect that cancels the applied field. Therefore, the total change produced by the applied field in this particular case has to sum cero. This effect is more clearly shown in Fig. 5 where the net increase in the average spin and orbital magnetic moments as a function of the applied field is shown.

4. Conclusion

In this contribution, a study of the magnetic properties of small Fe clusters was reported. The calculation was performed within an *ab initio* method that includes spin-orbit coupling. Our results for the spin and orbital magnetic moments in the different atomic environments, clearly show the dependence of the cluster magnetic properties on the size and

geometry. We also reported on the effect that applied external magnetic fields produce.

With our method, a more realistic treatment of the various electronic levels was possible. Nevertheless, a drawback from our approximation must be noted, since it is necessary to impose boundary conditions. This approximation usually overestimates the role of the interaction between electrons in different atomic states, producing finite bandwidths. In particular, the population of the p- and f-levels may be exaggerated.

A comparison of our results with photoelectron spectroscopy studies seems to validate the geometrical stucture assumed, except for the 15-atom cluster, where important deviations from the bcc structure may be present.

We expect that our results may motivate further experiments to characterize in a more detailed way the magnetic properties and their crucial dependence on the local environment dependence.

Acknowledgements

This work was partially funded by PROMEP-SEP-CA230. FAG acknowledges the spanish Ministry of Education and Science for a sabbatical Grant SAB-2004-0129.

∗ On sabbatical from: Instituto de Física, Universidad Autónoma de San Luis Potosí, 76240, San Luis Potosí, México.

1. S.N. Khana and S. Linderoth, *Phys. Rev. Lett.* **67** (1991) 742.
2. W.A. de Heer, P. Milani, and A. Châtelain, *Phys. Rev. Lett.* **65** (1990) 488.
3. I.M.L. Billas, A. Châtelain, and W.A. de Heer, *Science* **265** (1994) 1682.
4. I.M. Billas, J.A. Becker, A. Châtelain, and W.A. de Heer, *Phys. Rev. Lett.* **71** (1993) 4067.
5. J.P. Bucker, D.C. Douglass, and L.A. Bloomfeld, *Phys. Rev. Lett.* **66** (1991) 3052.
6. D.C. Douglass, A.J. Cox, J.P. Bucker, and L.A. Bloomfeld, *Phys. Rev. B* **47** (1993) 12874.
7. S.E. Apsel, J.W. Emmert, J. Deng, and L.A. Bloomfeld, *Phys. Rev. Lett.* **76** (1996) 1441.
8. S. Bouarab, A. Vega, J.A. Alonso, and M.P. Iñiguez, *Phys. Rev. B* **54** (1996) 3003.
9. O. Diéguez, M.M.G. Alemany, and C. Rey, *Phys. Rev. B* **63** (2001) 205407.
10. P. Bobadova-Parvanova, K.A. Jackson, S. Srinivas, and M. Horoi, *Phys. Rev. B* **66** (2002) 195402.
11. M. Castro, Ch. Jamorski, and D.R. Salahub, *Chem. Phys. Lett.* **271** (1977) 133.
12. M. Castro, *Int. J. Quantum Chem.,* **64** (1997) 223.
13. L.-S. Wang, X. Li, and H.-F. Zhang, *Chem. Phys.* **262** (2000) 53.
14. F. Brouers, F, Gautier, and J. van de Rest, *J. Phys. F,* **5** (1975) 975.
15. J.A. Franco, A. Vega, and F. Aguilera-Granja, *Phys. Rev. B* **60** (1999) 434.
16. P.J. Jensen and K.H. Bennemann, *Z. Phys. D* **21** (1991) 349; **35** (1995) 723.
17. F. Aguilera-Granja, J.M. Montejano-Carrizales, and J.L. Morán-López, *Phys. Lett A* **242** (1998) 255; *Solid State Commun.,* **107** (1998) 25.
18. O. Špir, M. Košuth, and H. Ebert, *J. Magnetism and Magnetic Materials* **272-276** (2004) 713.
19. O.B. Christensen and M.L. Cohen, *Phys. Rev. B,* **47** (1993) 643.
20. Cerius2, Version 4.0, Molecular Simulations Inc., San Diego CA, 1999.
21. J. Harris,*Phys. Rev. B* **31** (1985) 1770.
22. A.H. MacDonald, W.E. Picket, and D.D. Koelling, *J. Phys. C* **13** (1980) 2675.
23. A.R. Williams, and J. Kübler, *Phys. Rev. B* **19** (1979) 6094.
24. J. Guevara, F. Parisi, A.M. Llois, and M. Weissmann, *Phys. Rev. B* **55** (1997) 13283.